ELSEVIER

Journal of Magnetism and Magnetic Materials 248 (2002) 258–267

journal of magnetism and magnetic materials

www.elsevier.com/locate/jmmm

Pulsed-field-remanence measurements on individual magnetotactic bacteria

Marianne Hanzlik[1], Michael Winklhofer[2], Nikolai Petersen*

Institut für Geophysik, Ludwig-Maximilians-Universität, Theresienstr. 41, D-80333 Munich, Germany

Received 28 March 2002

Abstract

We measured pulsed-magnetic-field remanences of individual cells of two types of magnetotactic bacteria. Wild-type magnetic vibrios displayed square remanence curves with the reversal field, H_{rev} reaching values up to 825 Oe (65.7 kA/m). We attribute the generally high values of H_{rev} to the elongated shape of the magnetosomes (length-to-width ratio, $e \approx 1.2$) and to the comparatively short distances between the magnetosomes (8 nm). Cells of the rod-shaped *Magnetobacterium bavaricum*, on the other hand, which frequently contain more than 600 magnetosomes per cell, could gradually be demagnetised; the coercivity of remanence, H_{cr} of individual cells always ranged between 600 and 700 Oe (47.7–55.7 kA/m). The non-square remanence curves of *M. bavaricum* reflect a distribution of elongations and interactions between adjacent strands of magnetosomes within the braid-like chains.

PACS: 75.50.Gg; 75.50.Tt; 75.60.Ej; 92.20.Pz

Keywords: Bacteriodrome; Wild-type magnetic vibrio; *Magnetobacterium bavaricum*; Biogenic magnetite; Template-based crystal growth

1. Introduction

Magnetotactic bacteria [1] are microorganisms which contain intracellularly produced crystals, usually made of magnetite (Fe_3O_4). These so-called magnetosomes are magnetic single-domain particles (50–100 nm in size) and typically arranged in chains, which act as compass needles and so enable the bacteria to orientate in the Earth's magnetic field [2,3]. The polarity of magnetic bacteria in the northern hemisphere normally is north-seeking, and, correspondingly, south-seeking in the southern hemisphere.

Magnetic bacteria have been found in all aquatic environments (see Ref. [4] for a review), and even in soils [5]. They all live under microaerophilic to anaerobic conditions. Magnetic bacteria differ widely in their cell morphologies

*Corresponding author. Tel.: +49-89-2180-4233; fax: +49-89-2180-4205.

E-mail address: petersen@geophysik.uni-muenchen.de (N. Petersen).

[1] Now at: Institut für Technische Chemie, I, Technische Universität München, Lichtenbergstr. 4, D-85748 Garching, Germany.

[2] Now at: School of Ocean and Earth Science, University of Southampton, Southampton Oceanography Centre, European Way, Southampton SO14 3ZH, UK.

0304-8853/02/$ - see front matter
PII: S0304-8853(02)00353-0

as well as in the morphology of their magnetosomes and number of chains per cell as could be shown by electron microscopy. The question now arises in which way these differences are reflected in the magnetic properties of individual cells. An elegant way to discriminate magnetic bacteria without electron microscopy is to subject them to increasing magnetic pulse fields and to observe the response in their swimming behaviour.

Penninga et al. [6] were the first to use this method. They applied magnetic pulses to cells of two different types of magnetic bacteria, the *Magnetospirillum magnetotacticum*, which contains only one chain of magnetite particles, and a non-cultured, rod-shaped bacterium with two chains of greigite (Fe_3S_4) crystals. For *M. magnetotacticum*, the absolute value of the remanent magnetic moment did not change during application of magnetic pulses of increasing amplitude, but reversed in one single step at a certain field strength (reversal field H_{rev} [3] about 320 Oe). The rod-shaped bacteria in Ref. [6] displayed a different magnetisation characteristic: individual cells could be gradually demagnetised, although H_{rev} values are similar to those of the spirilla.

Apart from a magnetic characterisation, the aim of our pulse studies was to investigate the magnetisation state of the magnetosome chains within a single bacterium, in particular, to test if all the individual magnetosomes are magnetised in one and the same direction. We used two different types of magnetic bacteria: a wild-type vibroid bacterium with one single chain of magnetosomes (Fig. 1), and *Magnetobacterium bavaricum* (MB), with three to five braid-like bundles of chains (Fig. 2a). Although a little elongated, the magnetosomes of the wild-type vibrios are similar in shape to the ones of *M. magnetotacticum*, used by Penninga et al. in their pulse experiments.

The second type of bacterium studied here, MB (Fig. 2a), is an extraordinary bacterium. Phylogenetically, it seems to form an individual bacteria group that is older than the proteobacteria [7], which all other known magnetic bacteria are

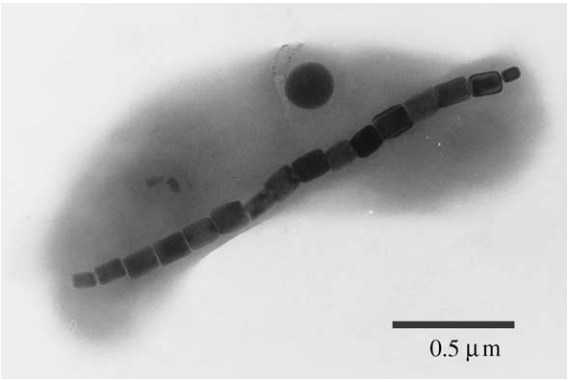

Fig. 1. Magnetic vibroid bacterium with a single chain of magnetosomes. The magnetosomes are slightly elongated and separated by small gaps of approx. 8 nm width. Scale bar 0.5 μm.

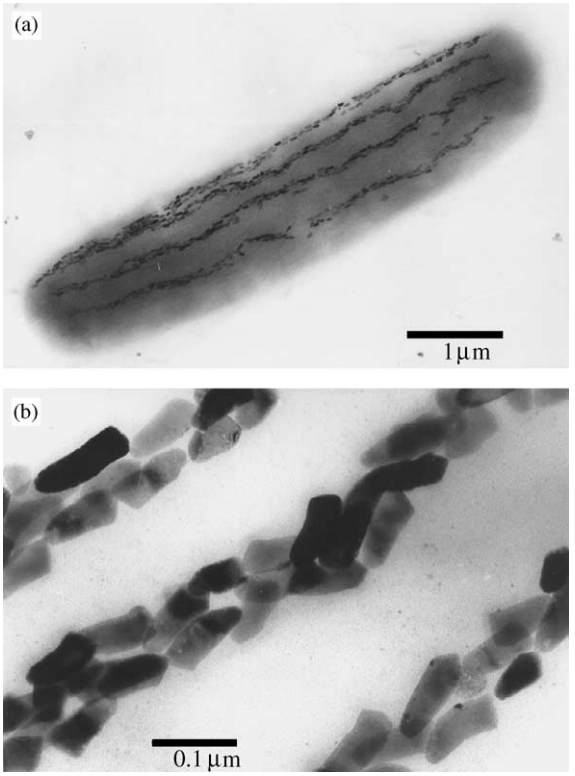

Fig. 2. *Magnetobacterium bavaricum.* (a) A cell contains 3 up to 5 bundles of magnetosome chains. The round globules consist of polysulfides. Scale bar 1 μm. (b) Internal structure of a chain bundle. Scale bar 0.1 μm.

[3] The magnetisation reversal field H_{rev} refers to the remanent magnetisation M_r ($H \approx 0$) of a sample, after exposure to a pulse magnetic field; in case the remanence is annulled by H_{rev}, the corresponding field is termed coercivity of remanence. In contrast, the magnetic field necessary to reverse the magnetisation $M(H)$ measured in an external field H is called coercive force, H_c.

assigned to. It is characterised by comparatively large, zeppelin-like cells up to 12 μm in length. An individual cell may contain more than 600 magnetosomes, which have a hook-like morphology and consist of magnetite. Because of their unusual morphology, magnetosomes of MB can easily be identified in magnetic extracts from sediments if present. The magnetosomes of MB are arranged in a peculiar way: two or three twisted strands of magnetosomes form a braid-like chain. It should be noted that the tips of the crystals do not all point in the same direction (Fig. 2b). About 80% point in the same direction, but 20%—randomly distributed over the chains—point in the opposite direction. From the magnetostatic point of view, a problem arises from the braid-like arrangement: If magnetised parallel to each other, neighbouring particles do not only occur in the energetically most favourable one-behind-each-other position, but also in a side-by-side position, which is energetically less favourable. It is therefore conceivable that one of the three strands of a chain bundle is polarised antiparallel to the main polarisation of the chain, thereby however considerably reducing the total magnetic moment.

In order to reveal the polarisation state within the chains and thus to decide between the above-mentioned two possibilities, we conducted pulsed-magnetic-field remanence measurements on individual bacteria.

2. Measurements and parameters

The investigation was conducted in our "bacteriodrome" (Fig. 3) [8,9], which consists of a light-microscope with video camera (M) surrounded by three independent Helmholtz-coil systems (C1–C3): pulsed-magnetic fields are applied with the Helmholtz-coil pair C1. The two Helmholtz pairs C2 produce a magnetic field rotating in the plane of the specimen (S) to guide the bacteria on a circular trajectory. The three outer Helmholtz pairs (C3), arranged perpendicular to each other, are used to neutralise the vertical component of the Earth's magnetic field, and to adjust a constant—usually planar—magnetic field (here called H_{app}). A similar system was described recently [10].

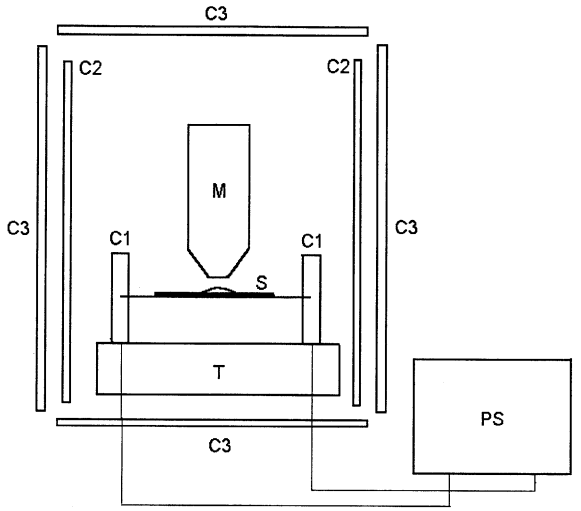

Fig. 3. Schematic outline of bacteriodrome, a light-microscope with video-camera surrounded by three independent systems of Helmholtz-coil pairs. The inner pair of coils was designed to generate magnetic pulses with maximum amplitudes of 3000 G. The pulse duration is 2 ms. M—microscope, S—specimen, T—microscope table, C1—pulse field coils, C2—Helmholtz-coils for the bacteriodrome, C3—field coils for compensation of the earth's magnetic field PS—pulse electronics.

After extraction and separation from the sediment, the magnetic bacteria were killed using formaldehyde vapour. During this process, most of the bacteria lost their flagellum. The natural remanent magnetic moment of each bacterium was then determined using the "rotating-field method" [8,9]. Then, the dead bacteria were aligned in a weak constant field H_{app} of about 1 Oe. The aligned cells were exposed to magnetic pulses of increasing magnitude, and of polarity opposite to H_{app}. After each pulse, the magnetic moment was determined by the rotating-field method as before. The magnitude of the pulse field ranged from 200 Oe to about 3000 Oe, the duration of a pulse is 2 ms.

3. Theoretical modelling

3.1. Switching fields

To interpret the characteristics of magnetisation reversals in magnetosome chains, we employ a

modified "chain-of-spheres" model. The original chain-of-spheres model was introduced by Jacobs and Bean [11, loc. cit. JB55] to explain why switching fields of highly elongated particles are much lower than predicted by the Stoner–Wohlfahrt (SW) theory [12]. While the magnetisation of an SW ellipsoid is constrained to rotate coherently during reversal (Fig. 4a, left) to overcome the shape-anisotropy barrier, the chain-of-spheres model allows for non-coherent reversal mechanisms. Assuming a symmetric-fanning mechanism (Fig. 4a, right), JB55 obtained switching fields in good accordance with experimental data.

The chain-of-spheres model used here is modified in the following aspects:

1. Unlike the spheres in the JB55 model, the magnetosomes in magnetic bacteria do not touch, but are separated by a finite distance, which reduces coercive fields [13].
2. In contrast to the magnetic spirilla examined in Ref. [6], magnetosomes of the investigated wild-type vibrios (Fig. 1), or of the rod-shaped MB (Fig. 2b) are elongated. We approximate magnetosomes of vibrios (typical length-to-width ratios range from $e = 1.2$–1.3) by prolate SW ellipsoids (Fig. 4b, left); the interaction integrals between two SW ellipsoids were computed numerically (see Ref. [14] for mathematical treatment).
3. The magnetisation in more elongated SD particles ($e \approx 2$) as those of MB, however, is expected to reverse not in unison. We therefore find it more appropriate to model these rod-shaped particles as (sub)-chains of spheres in the chain-of-spheres system (Fig. 4b, right).
4. The spheres in JB55 were without crystal anisotropy. For magnetite crystals with aspect ratio close to unity, it is necessary to take into account magnetocrystalline anisotropy in order not to underestimate the switching fields. Analytical formulae for the switching fields of chains of spheres with uniaxial magnetocrystalline anisotropy are available in the literature [15]. However, we used cubic magnetocrystalline anisotropy, with the $\langle 1\,1\,1 \rangle$ easy axis of the crystals lying in the direction of the chain, which is usually the case for magnetosomes made from magnetite.

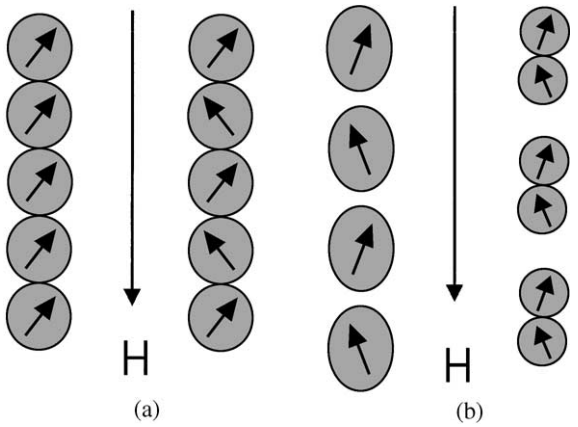

Fig. 4. (a) Mechanisms for magnetisation reversal considered in the chain-of-spheres model by JB55: coherent rotation (left), and symmetrical fanning (right). (b) Modified chain-of-spheres model to simulate the reversal characteristics of magnetosome chains: adjacent particles do not touch each other, the particles are elongated, and possess a cubic crystallographic shape anisotropy with the [1 1 1] easy axis oriented along the chain direction. Less elongated magnetosomes are modelled as SW ellipsoids (left); more elongated magnetosomes are approximated by sub-chains of spheres (right).

3.2. Uniform polarity in a chain bundle?

Besides the reversal characteristics of magnetosome chains, the other question to be treated theoretically is related to the polarity of the individual strands of a chain bundle in MB. It needs to be evidenced that two or three adjacent strands can all have one and the same polarity in a bundle without being driven apart from each other by magnetostatic repulsion forces. At first glance, this statement seems somewhat counterintuitive insofar as it requires considerable force to hold two bar magnets against each other in the highly unstable parallel (side-by-side) position. On the other hand, a magnetosome chain is not comparable in all aspects to a simple bar magnet as adjacent magntetosomes are separated by certain gaps. In the following, we shall elucidate the contribution of the gaps to the mechanical stability of chain bundles with uniform polarity. To illustrate the physical principle, we use a simple schematic system consisting of three

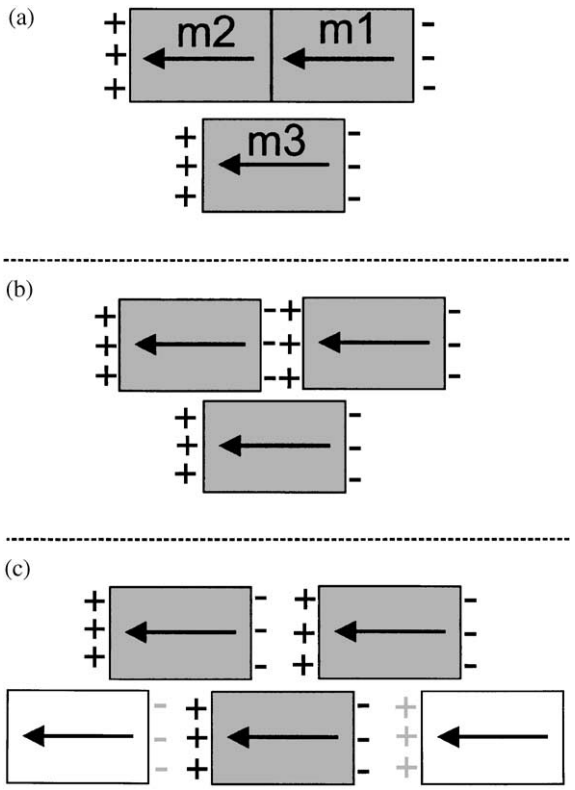

Fig. 5. Sketch to illustrate the importance of the magnetosome gaps for the formation of double chains (see detailed explanation in Section 3.2). As the gap widens, surface charges of opposite polarity approach each other in the side-by-side position, thereby enabling the formation of double chains.

magnetosomes arranged as shown in Fig. 5. It is sufficient to consider the interactions of the magnetically charged faces of m3, m3+ and m3−, with those of m1 and m2; the interaction between m1 and m2 is not relevant here. Without a gap between m1 and m2 (Fig. 5a), the surface charge closest to m3+, m2+, is of the same sign (polarity); the interaction therefore is repulsive. On introducing a small gap between m1 and m2 (Fig. 5b), a new pair of surfaces originates between m1 and m2, facing each other, with opposite polarities. For a very narrow gap, the new surfaces m1+ and m2− are so close together that the attractive interaction between m3+ and m2− is weakened by charge m1+. As the gap widens (Fig. 5c), however, the repulsive effect of m1+ declines and, at the same time, the attraction between m3+ and m2− strengthens; altogether, m3 and m2 become magnetically bound together. The same consideration applies to the pair m3 and m1. Following that principle, two adjacent chains with the same magnetisation can be realised (indicated by the open "magnetosomes" in Fig. 5c).

For a quantitative treatment, we employ a model similar to the one we developed earlier to calculate the repulsion force between two magnetosome chains lying on opposite sides within a magnetic coccus [16]. Here, we compute the interaction energy between three adjacent magnetosome chains polarised in the same direction as a function of their mutual displacements parallel to the chain axis, starting from the configuration where the three chains are aligned to each other. A continuous variation in one longitudinal displacement is equivalent to shifting one magnetosome chain past the other ones along the chain axis. Each energy surface is computed for a given gap size g and magnetosome elongation e, which both are constant over the chains, and a given lateral separation (offset) of the chains. Several energy surfaces are calculated to determine the influence of the parameters g and e. The uniform-polarity-in-chains hypothesis is verified if energy minima are found for chain geometries similar to the ones observed in bacteria.

4. Results and discussion

Fig. 6a shows a typical pulsed-magnetic-field remanence curve for a vibroid bacterium, containing one chain (Fig. 1). Although displaying a higher reversal field, the remanence curve is quite similar to those reported for *Magnetospirilla* in Ref. [6]. The magnetic moment remains nearly unchanged during application of increasing pulse fields until it reverses in a single step at about 825 Oe. This very high reversal field—compared to the 320 Oe determined for spirilla by Penninga et al. [6]—is due to the slightly elongated shape of the magnetosomes ($e \approx 1.2 \ldots 1.3$) and the very short distances (8 nm) between adjacent crystals.

Fig. 6b shows the calculated dependence of the reversal field on the gap width g between adjacent

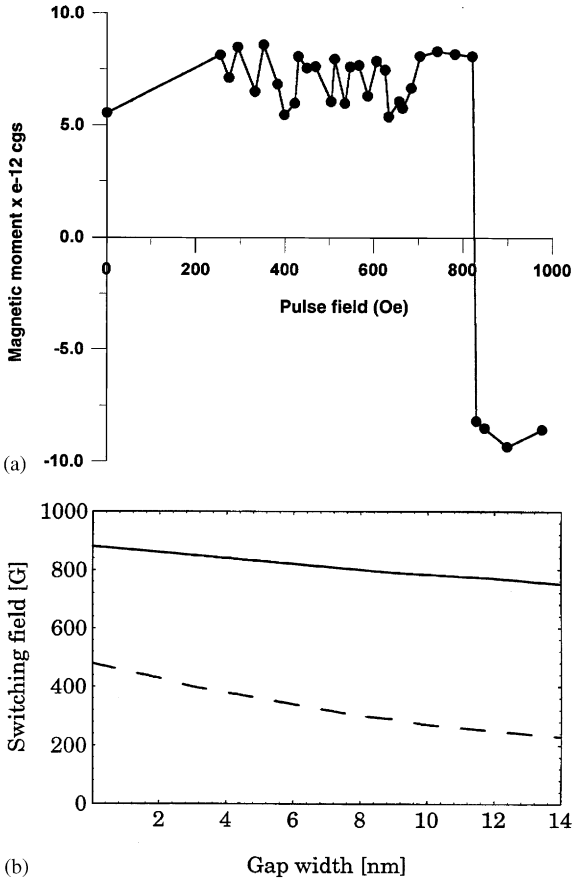

Fig. 6. (a) Pulsed-magnetic remanence curve for an individual cell of a wild-type magnetic vibrio. The remanent magnetic moment remains nearly unchanged during the application of increasing pulse fields until it reverses in a single step at about 825 Oe. (b) Calculated reversal field for a chain of ten prolate spheroids for slightly elongated (solid line, $e = 1.3$) and equidimensional magnetosomes (broken line, $e = 1.0$) as a function of the gap width g, according to the modified chain-of-spheres model (Fig. 4b, left).

particles according to the modified chain-of-spheres model: It can be seen that (1) chains of elongated particles have much higher values of H_{rev} than those composed of equidimensional particles; (2) the decrease of H_{rev} with g is more pronounced for equidimensional crystals than for elongated ones, whereas the chain length turned out to be of minor influence.

A completely different magnetisation behaviour is displayed by MB (Fig. 7). With increasing

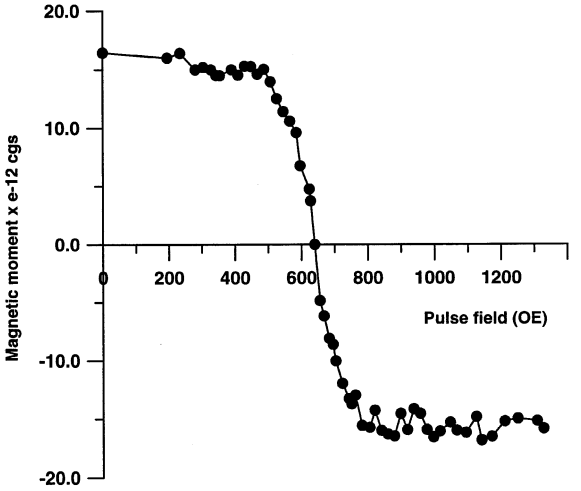

Fig. 7. Remanence curve measured on an individual cell of MB. The magnetic moment decreases with increasing pulse field (opposite polarity), the absolute value after application of 1500 Oe (150 mT) is similar to the one before the pulse-field series.

strength of the antiparallel pulse field, the magnetic moment decreases until it reaches zero. Further pulse-field application results in increasing values of the magnetic moment, but now of opposite sign, until saturation is achieved. The magnetisation reversal field of 670 Oe is distinctively lower than expected for the markedly elongated magnetosomes ($e = 1.7-2.5$), which is presumably due to interaction between crystals adjacent in the side-by-side position. The measurements show that—in contrast to vibrios and sprirrilla—cells of MB can be demagnetised. This may have two reasons: (1) the sometimes irregular arrangement of the magnetosomes within the chains, which favours the reversal of crystals with more suitable orientations with respect to the pulse field, (2) the varying elongations of juvenile ($e = 1$) and mature ($e < 3$) magnetosomes, which results in a certain distribution of coercive forces. As the pulse field increases, more and more individual switching fields are exceeded, and the magnetisation of the corresponding crystal reverses.

In order to reveal the polarities of individual chains, cells of the MB were exposed to increasing pulse fields, this time applied parallel to the (weak) guiding field, H_{app}. Again the magnetic moment

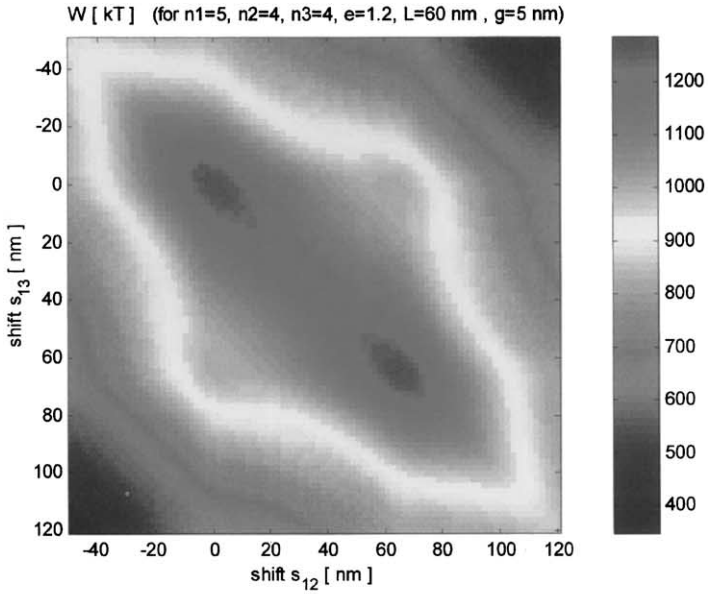
W [kT] (for n1=5, n2=4, n3=4, e=1.2, L=60 nm , g=5 nm)
shift s13 [nm]
shift s12 [nm]
-40
-20
0
20
40
60
80
100
120
1200
1100
1000
900
800
700
600
500
400

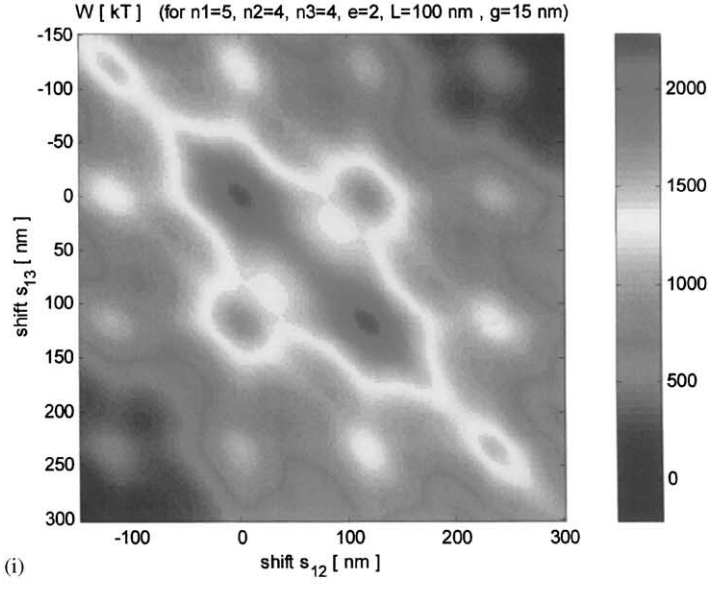
W [kT] (for n1=5, n2=4, n3=4, e=2, L=100 nm , g=15 nm)
shift s13 [nm]
shift s12 [nm]
-150
-100
-50
0
50
100
150
200
250
300
2000
1500
1000
500
0

(i)

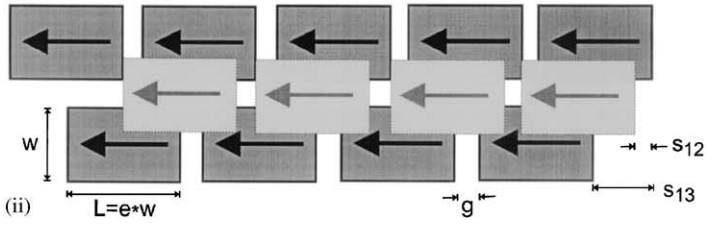
W
L=e*w
g
s12
s13

(ii)

was measured after each pulse step, but not even the maximum field of 3000 Oe was able to noticeably increase the remanent magnetic moment. Therefore, the natural magnetic remanence of the cells corresponds to the maximally possible remanence. That is, all bundles of chains as well as the individual chains of a bundle are magnetised (sub)parallel to the bulk magnetisation of a cell. Otherwise we would have seen an increase due to switching in chains with polarity antiparallel to the main polarity.

This experimental result can be supported theoretically as well. Fig. 8 shows the energies for various chain configurations in a so-called "energy-landscape representation" (see Section 3.2). Each point on such a two-parametric surface represents a particular arrangement of the three magnetosome chains, the corresponding energy is given by the level of the contour line through that point. The undulations on the energy landscape are due only to shifting the chains relative to each other. The landscape shown in Fig. 8a, was calculated for chains consisting of ideal magnetosomes with a length-to-width ratio of $e = 2$, the gap width was taken as $g = 15$ nm. These values are typical of MB. Two energetically stable triple-chain configurations exist for this case as indicated by the minima at ($s12$, $s13$) = (20 nm, 100 nm). The situation changes distinctly when reducing the elongation to $e = 1.2$ and the gap width to $g = 5$ nm (Fig. 8b). Obviously, the gaps are too narrow to enable a stable triple-chain configuration.

The unusual shape of the magnetosomes of MB lets us suggest that crystal growth of the magnetosomes in MB is governed by a different mechanism to the one postulated for other species such as spirilla, cocci, or vibrios. The standard theory there is based on membrane-bounded vesicles of special morphology prior to the crystals [17–19]. In such vesicles, the magnetosomes precipitate and grow until they touch the membrane and further growth is inhibited. So the crystal morphology as well as the maximal crystal size are determined by the vesicle form and size.

In the case of the peculiar magnetosome shape of MB, however, it is not easy to imagine a fitting vesicle structure. Using different preparation techniques, we tried to find magnetosome-enclosing vesicles [20]. Yet, we were not able to detect any membrane surrounding the magnetite particles. We therefore suggest a different growth mechanism based on templates. This idea originated from the observation of a dark layer at the crystal base, which could only be seen in one special orientation in the TEM (Fig. 9a). Instead of membrane-enclosed vesicles, we postulate a tree-like template structure for MB (Fig. 9b). Here, the direction of the crystal growth—tip up or down—depends on the orientation given by the template.

Another peculiarity of MB is the prominent kink of the magnetosomes (from [1 1 1] to probably [1 1 4]) which always occurs in mature crystals and which we attribute to an interaction with the magnetic fields of the nearest neighbours, influenced by the magnetic orientation of neighbouring magnetosomes. These are all polarised in the same direction, which results in a repulsive force between side-by-side neighbours attempting to rotate the crystals out of the chain axis. Our conjecture is supported by the observation that

Fig. 8. Energy surface for an idealised triple chain of magnetosomes (see small sketch). The three adjacent strands are polarised parallel to each other, in the chain direction. The parameter $s12$ represents the shift of strand 2 with respect to strand 1, and $s13$ the shift between strand 3 and 1. The energy is expressed in units of the thermal energy, kT (k—Boltzmann's constant, T—temperature, here 300 K). $n1, n2, n3$, are the respective numbers of magnetosomes per chain, here 5,4,4. Interaction energies between the magnetically charged surfaces are calculated using the formula given in Ref. [21]. Perfect alignment of the three strands (i.e., $s12 = s13 = 0$) is related to a local energy maximum, and therefore represents a highly unstable configuration. However, on shifting the strands relative to each other in axial direction by less than a magnetosome length, a stable arrangement can be achieved, which is represented in a) by the minima around $s12 = 20$ nm and $s13 = 100$ nm (and vice versa, because of the symmetry between chains 2 and 3). The small sketch shows the corresponding arrangement. (b) If, however, gap width and elongation are chosen too small, no physically stable triple-chain configuration can be realised.

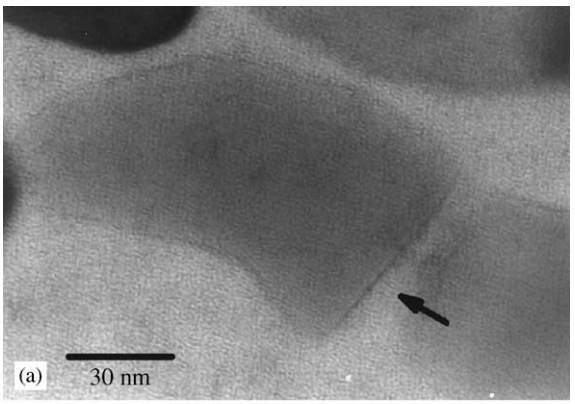

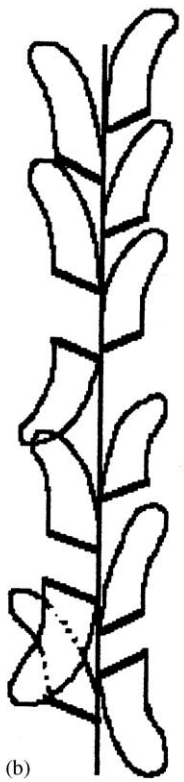

Fig. 9. (a) Detailed view of a single magnetosome of MB (scale bar 30 nm). A dark layer at the crystal base can be seen (arrow), which we consider a template, where crystal growth may initiate. (b) Suggested tree-like, template-controlled growth for magnetosomes to form a bundle of magnetosomes.

such kinks do not occur in magnetic bacteria in which spearhead-shaped magnetosomes are arranged in single chains (Fig. 10).

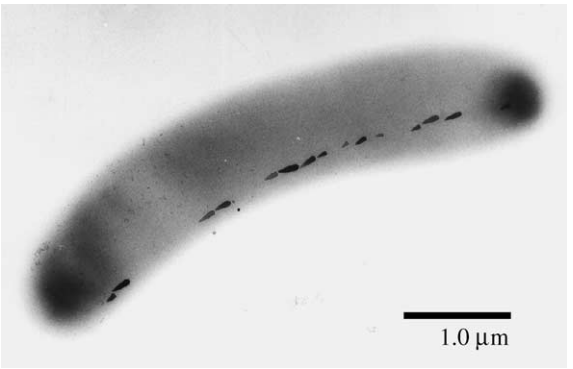

Fig. 10. A wild-type magnetic vibrio with a single chain of "spearhead"-shaped magnetosomes. In contrast to the magnetosomes of MB, which occur in bundles and develop kinks during growth, those magnetosomes remain straight. Scale bar is 1 μm.

5. Conclusions

The pulse-magnetic field method is suitable to magnetically characterise cells of different types of magnetotactic bacteria and to distinguish them.

The observed values for the reversal fields can be well explained with a modified chain-of-spheres model. The high reversal fields displayed by wild-type vibrios reflect the elongated magnetosome shape (length-to-width ratio between 1.2 and 1.3).

For MB, we could show both experimentally and theoretically, that the polarity in bundles of magnetosome chains is uniform. In contrast to the wild-type vibrios these cells can (nearly) be demagnetised because of a distribution of coercive forces due to a distribution of magnetosome elongations in a cell.

As MB is phylogenetically older than all the other magnetic bacteria classified so far, the growth mechanism of the magnetosomes may differ as well. We suggest that template-based crystal growth is not yet optimised as compared to the vesicle-based growth in all other magnetic bacteria.

Acknowledgements

This investigation was supported by the Deutsche Forschungsgemeinschaft.

References

[1] R.P. Blakemore, Science 190 (1975) 377.
[2] A. Kalmijn, R.P. Blakemore, in: K. Schmidt-Koenig, W.T. Keeton (Eds.), Animal Migration, Navigation and Homing, Springer, Berlin, 1978.
[3] R.B. Frankel, R.P. Blakemore, J. Magn. Magn. Mater. 15–18 (1980) 1562.
[4] D.A. Bazylinski, B.M. Moskowitz, in: J.F. Banfield, K.H. Nealson (Eds.), Geomicrobiology, Mineral Society of America, Washington, 1997, pp. 181–223.
[5] J.W.E. Fassbinder, H. Stanjek, H. Vali, Nature 343 (1990) 181.
[6] I. Penninga, H. de Waard, B.M. Moskowitz, D.A. Bazylinski, R.B. Frankel, J. Magn. Magn. Mater. 149 (1995) 279.
[7] S. Spring, R. Amann, W. Ludwig, K.H. Schleifer, H. van Gemereden, N. Petersen, Appl. Environ. Microbiol. 59 (1993) 2397.
[8] N. Petersen, D.G. Weiss, H. Vali, in: F.J. Lowes, et al., (Eds.), Geomagnetism and Paleomagnetism, Kluwer Academic Press, Dordrecht, Netherlands, 1989, pp. 231–241.
[9] B. Steinberger, N. Petersen, H. Petermann, D. Weiss, J. Fluid Mech. 213 (1994) 189.
[10] H. de Waard, J. Hilsinger, R.B. Frankel, Rev. Sci. Instr. 72 (2001) 2724.
[11] I.S. Jacobs, C.P. Bean, Phys. Rev. 100 (1955) 1060.
[12] E.C. Stoner, E.P. Wohlfarth, Philos. Trans. R. Soc. (London) A 240 (1948) 599.
[13] B.M. Moskowitz, R.B. Frankel, P.J. Flanders, R.P. Blakemore, B.B. Schwartz, J. Magn. Magn. Mater. 73 (1988) 289.
[14] E.P. Wohlfarth, Proc. R. Soc. (London) Ser A 232 (1955) 208.
[15] H.J. Richter, J. Magn. Magn. Mater. 154 (1996) 263;
Y. Ishi, M. Sato, J. Appl. Phys. 59 (1986) 880.
[16] M. Hanzlik, M. Winklhofer, N. Petersen, Earth Planet. Sci. Lett. 145 (1996) 125.
[17] D. Balkwill, D. Maratea, R.P. Blakemore, J. Bacteriol. 141 (1980) 1399.
[18] Y.A. Gorby, T.J. Beveridge, R.P. Blakemore, J. Bacteriol. 170 (1988) 834.
[19] D. Schüler, E. Baeuerlein, J. Phys. IV 7 (1997) 647.
[20] M. Hanzlik, Elektronenmikroskopische und magnetomineralogische Untersuchungen an magnetotaktischen Bakterien des Chiemsees und an babteriellem Magnetit eisenreduzierender Bakterien, Dissertation, LMU München, Germany, 1999.
[21] P. Rhodes, G. Rowlands, Proc. Leeds Philos. Lit. Soc. 6 (1954) 191.